

# PROCEEDINGS OF SPIE

[SPIDigitalLibrary.org/conference-proceedings-of-spie](https://spiedigitallibrary.org/conference-proceedings-of-spie)

## Evaluation of Mueller matrix of achromatic axially symmetric wave plate

Toshitaka Wakayama, Kazuki Komaki, Israel Vaughn, J. Scott Tyo, Yukitoshi Otani, et al.

Toshitaka Wakayama, Kazuki Komaki, Israel J. Vaughn, J. Scott Tyo, Yukitoshi Otani, Toru Yoshizawa, "Evaluation of Mueller matrix of achromatic axially symmetric wave plate," Proc. SPIE 8873, Polarization Science and Remote Sensing VI, 88730P (27 September 2013); doi: 10.1117/12.2023849

**SPIE.**

Event: SPIE Optical Engineering + Applications, 2013, San Diego, California, United States

# Evaluation of Mueller matrix of achromatic axially symmetric wave plate

Toshitaka Wakayama\*<sup>a</sup>, Kazuki Komaki<sup>a, b</sup>, Israel J. Vaughn<sup>c</sup>, J. Scott Tyo<sup>c</sup>,  
Yukitoshi Otani<sup>b</sup>, Toru Yoshizawa<sup>d</sup>

<sup>a</sup>School of Biomedical Engineering, Saitama Medical University, Hidaka, Saitama 350-1241, Japan;

<sup>b</sup>Center for Optical Research and Education, Utsunomiya University, Utsunomiya, Tochigi 321-8585, Japan;

<sup>c</sup>College of Optical Sciences, University of Arizona, Tucson, AZ 85721, USA;

<sup>d</sup>NPO 3D Associates, Turumi, Yokohama, Kanagawa 230-0078, Japan.

## ABSTRACT

Axially symmetric polarized beams have attracted great interest recently in the field of optics. There have been several viable proposals concerning axially symmetric polarizers, also referred to as radial polarizers. In contrast, proposals for axially symmetric wave plates have strong dependence on wavelength. Moreover, the structure of the axially symmetric wave plates inherently introduces spatial dispersion. As a solution to these problems, we propose an achromatic axially symmetric wave plate based on internal Fresnel reflection that does not introduce spatial dispersion. It is possible to generate the achromatic axially symmetric polarized beam. In this paper, we show the principle of the achromatic axially symmetric wave plate and the evaluation results of the optical element using a Mueller matrix polarimeter.

**Keywords:** axially symmetrical polarized beam, Fresnel reflection

## 1. INTRODUCTION

In recent years, polarization vortices have attracted great interest similar to optical vortices in the field of optical sciences [1, 2]. When the phase of the polarization vortex is nearly in-phase on the beam area, polarization states are axially symmetric. Therefore, an optical beam producing a polarization vortex is called an axially symmetric polarized beam, and its intensity distribution is also doughnut shaped. One interesting paper has proposed to generate a longitudinal electric field by focusing the axially symmetric polarized beam through an objective lens with a high numerical aperture creating a longitudinal component of the electric field. [3]. The resulting longitudinal electric field should be able to accelerate electrons [4]. Other proposed applications include laser processing, super-resolution microscopes, and laser trapping [5–7]. To generate the axially symmetric polarized beam, most published research has proposed using liquid crystals, photonic crystals, nano-structures, and optical cavities [8–13]. Particularly, proposals based on photonic crystals and nano-structures have been used to fabricate axially symmetrical wave plates. However, conventional axially symmetric wave plates have technical problems, including spatial dispersion and wavelength-dependence. To overcome these problems, we have developed axially symmetric wave plates based on internal Fresnel reflections [14]. The advantage of our proposal is that our wave plate can perform achromatically. We have shown to generate the axially symmetric polarized beam with higher order, fundamentally and experimentally [15]. In this research, we fabricated the axially symmetric wave plate using SiO<sub>2</sub> as an optical material. In this paper, we show specific data of the wave plate, and we evaluate the wave plate using a dual rotating Mueller matrix polarimeter. The wave plate performance is in good agreement with the theoretical predictions of its Mueller matrix distribution. Moreover, we discuss the polarization properties of the achromatic axially symmetric wave plate.

\*Toshitaka Wakayama; phone 81 42 984-0686; fax 81 42 984-4819; [wakayama@saitama-med.ac.jp](mailto:wakayama@saitama-med.ac.jp)

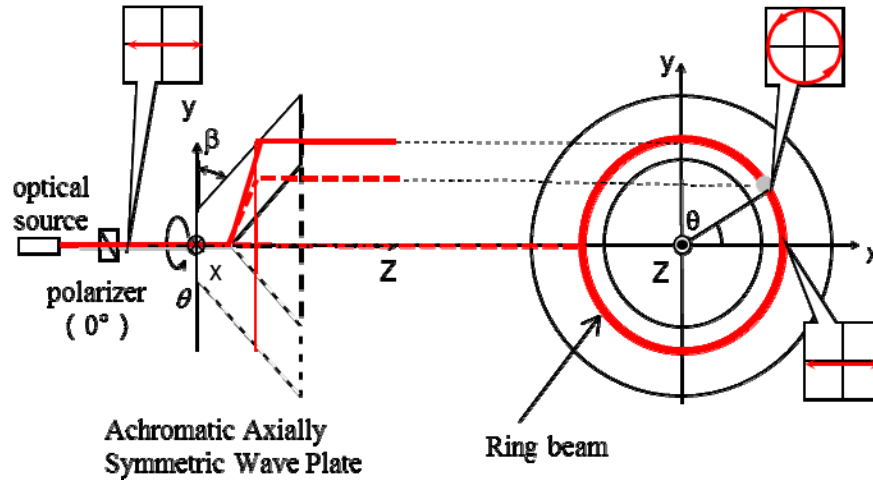


Fig.1 Optical configuration of achromatic axially symmetric wave plate[14]

## 2. PRINCIPLE OF ACHROMATIC AXIALLY SYMMETRIC WAVE PLATE

Figure 1 shows an optical configuration of an achromatic axially symmetric wave plate based on internal Fresnel reflection. A light beam is transmitted through a polarizer set at  $0^\circ$  before incidence on the achromatic axially symmetric wave plate. The wave plate has basically a concave conical surface similar to a Fresnel rhomb rotated about an optical axis,  $z$ . The reflected beam on the top of the concave conical surface becomes a cone beam. Moreover, the cone beam reflects on the slope of the wave plate. The output beam becomes a ring beam because this reflection is omnidirectionally generated along the optical axis. Two internal Fresnel reflections can produce a phase difference of  $\Delta$  in the  $p$ - $s$  orthogonal polarization states:

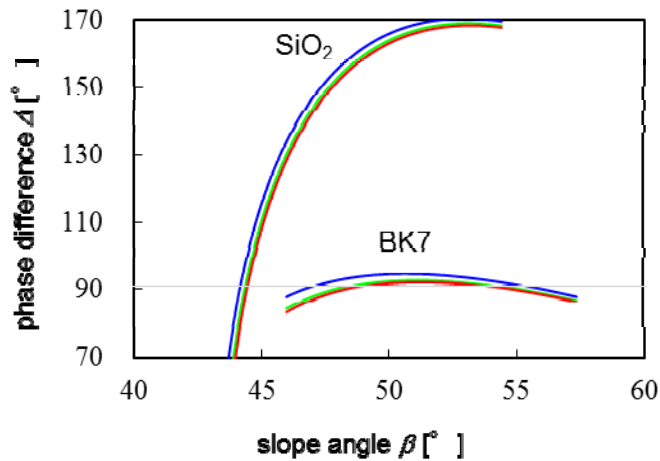
$$\Delta = 4 \tan^{-1} \frac{\sqrt{n^2 \sin^2 \beta - 1}}{n \sin \beta \tan \beta} \quad (1) \quad [15,16]$$

where  $n$  and  $\beta$  are the index of the achromatic axially symmetric wave plate material and the slope angle of the achromatic axially symmetric wave plate, respectively. From this equation, we can easily understand how the phase difference relates to refractive index  $n$  and slope angle  $\beta$ . Although refractive index  $n$  depends on the wavelength  $\lambda$ , the slope angle  $\beta$  is independent of the wavelength. Therefore, we have to take into account the wavelength dependence of the refractive index, written  $n(\lambda)$ . Additionally the azimuthal angle of the wave plate changes along the angle  $\theta$ .

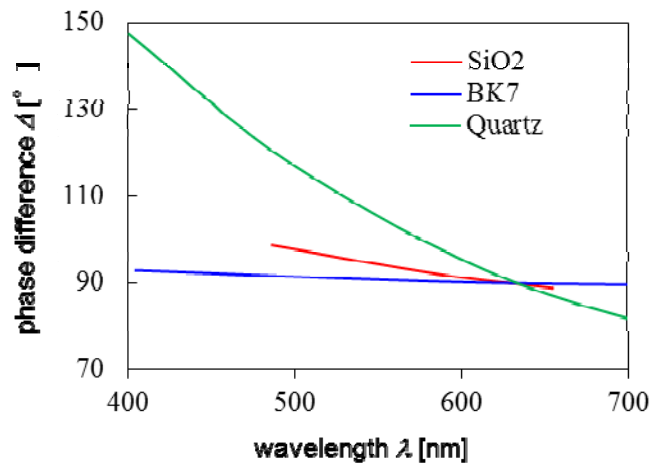
If the phase difference  $\Delta$  equals  $90^\circ$ , the optical element acts as an achromatic axially symmetric quarter-wave plate. The polarization states of the output beam vary around the ring and correspond to the polarization states of a rotating quarter-wave plate. Using the phase difference  $\Delta$ , the Mueller matrix of the axially symmetric wave plate can be expressed in the  $x$ - $y$  coordinate system as

$$M(x,y) = \begin{bmatrix} 1 & 0 & 0 & 0 \\ 0 & \cos^2 2\theta + \sin^2 2\theta \cos \Delta & \sin 2\theta \cos 2\theta (1 - \cos \Delta) & -\sin 2\theta \sin \Delta \\ 0 & \sin 2\theta \cos 2\theta (1 - \cos \Delta) & \sin^2 2\theta + \cos^2 2\theta \cos \Delta & \cos 2\theta \sin \Delta \\ 0 & \sin 2\theta \sin \Delta & -\cos 2\theta \sin \Delta & \sin \Delta \end{bmatrix} \quad (2) \quad [14]$$

where  $\theta$  is the angle shown in Fig. 2,  $\theta = \tan^{-1}(y/x)$ .



(a) Slope angle dependence



(b) Wavelength dependence

Fig.2 Properties of phase difference of axially symmetric wave plate

### 3. NUMERICAL SIMULATION OF INTERNAL FRESNEL REFLECTION

We determined the slope angle  $\beta$  to obtain the achromatic phase difference in the visible wavelength. In this paper, we simulated the phase difference of Fresnel reflection for the  $\text{SiO}_2$ , using indices  $n = 1.46314$  ( $\lambda = 486 \text{ nm}$ : blue line),  $n = 1.45847$  ( $\lambda = 587 \text{ nm}$ : green line), and  $n = 1.45737$  ( $\lambda = 656 \text{ nm}$ : red line), and that for BK7, using indices  $n = 1.53024$  ( $\lambda = 404 \text{ nm}$ : blue line),  $n = 1.5168$  ( $\lambda = 587 \text{ nm}$ : green line), and  $n = 1.51289$  ( $\lambda = 706 \text{ nm}$ : red line).

Figure 2(a) shows properties of the slope angle dependence. The blue, green, and red lines indicate the phase differences for the indices at 486 nm, 587 nm, and 656 nm, respectively. We obtained that when the achromatic slope angle  $\beta = 44.4^\circ$ , the phase difference is almost  $90^\circ$ . Figure 2(b) shows properties of the wavelength dependence of phase difference of different materials such as  $\text{SiO}_2$ , BK7 and quartz. In the case of quartz, the phase difference is due to the wavelength dependence on the birefringence. In our calculation, the BK7 gave good performance for the visible spectrum. The variation in the phase difference of BK7 is within  $\pm 1.7^\circ$  in visible wavelength range. If we use materials with less index dispersion, this variation becomes smaller. On the other hand, the phase difference for  $\text{SiO}_2$  is larger than the BK7 and smaller than the quartz. However,  $\text{SiO}_2$  is suitable to use as the optical material if the achromatic axially symmetric quarter wave plate is designed for coaxial optics.

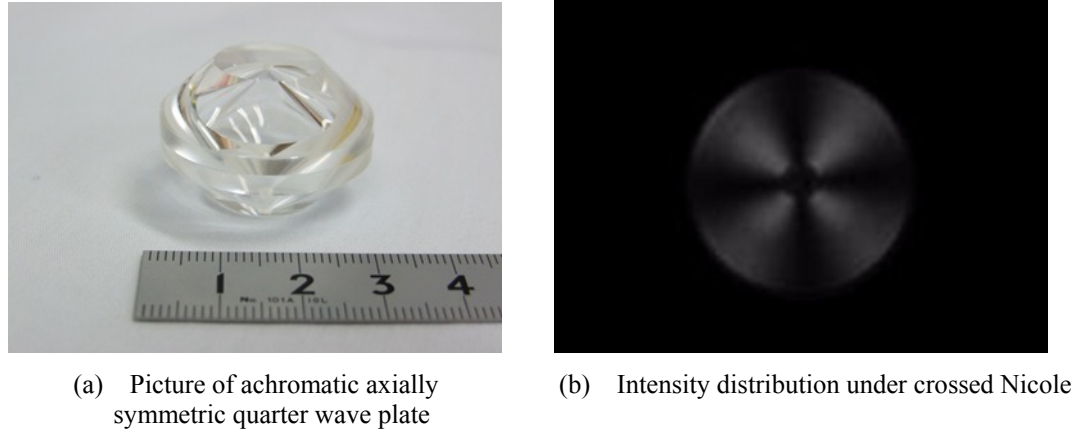


Fig.3 Achromatic axially symmetric wave plate

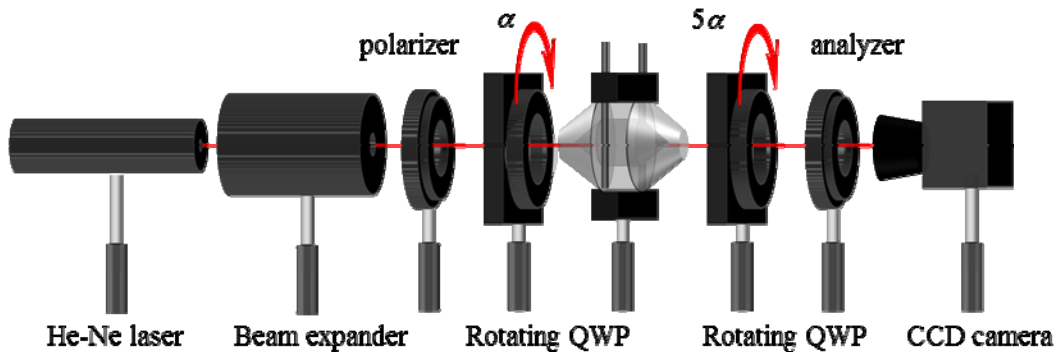


Fig.4 Dual rotating Mueller matrix polarimeter

#### 4. EXPERIMENTAL RESULTS

Figure 3(a) shows a pair of achromatic axially symmetric quarter wave plates. SiO<sub>2</sub> (Shinetsu Sekiei Co. Ltd.) is employed as an optical material. They are 30 mm in diameter and 20 mm long. The achromatic axially symmetric quarter wave plate is manufactured using a glass lathe and the polishing was processed by Natsume Optical Corp., precisely and carefully. Figure 3(b) shows the intensity distribution under the crossed Nicolé polarizers. According to this figure, we easily found that the generated beam has a doughnut-shaped intensity distribution and the azimuthal angle is changing axial-symmetrically. By rotating the analyzer in this evaluation system, we investigate whether the output beam is axially symmetric. The intensity distribution changed as a function of the rotation angle of the analyzer. From these results, it is clear that the wave plate can generate an axially symmetric polarized beam. The dark area indicates a linearly polarized beam and the bright area represents an elliptical polarized beam. The change of polarization states along the angle  $\theta$  of the wave plate correspond to polarization states obtained by rotating a quarter wave plate in the time domain.

For the present study, we employed a He-Ne laser, a beam expander ( $\times 10$ ), two Glan–Thompson polarizers, two rotating quarter wave plates and a CCD camera. Figure 4 shows the evaluation system of Mueller matrix of the achromatic axially symmetric wave plate using a dual rotating Mueller matrix polarimeter. The first and second quarter wave plates are rotating at the ratio 1:5, respectively. In this experiment, we captured 60 frames of the intensity distribution by the CCD camera. The CCD camera has  $640 \times 480$  pixels with 8 bits gray scale.

Figure 5 shows Mueller matrices distribution from  $m_{00}$  to  $m_{33}$  of the achromatic axially symmetric quarter wave plate.

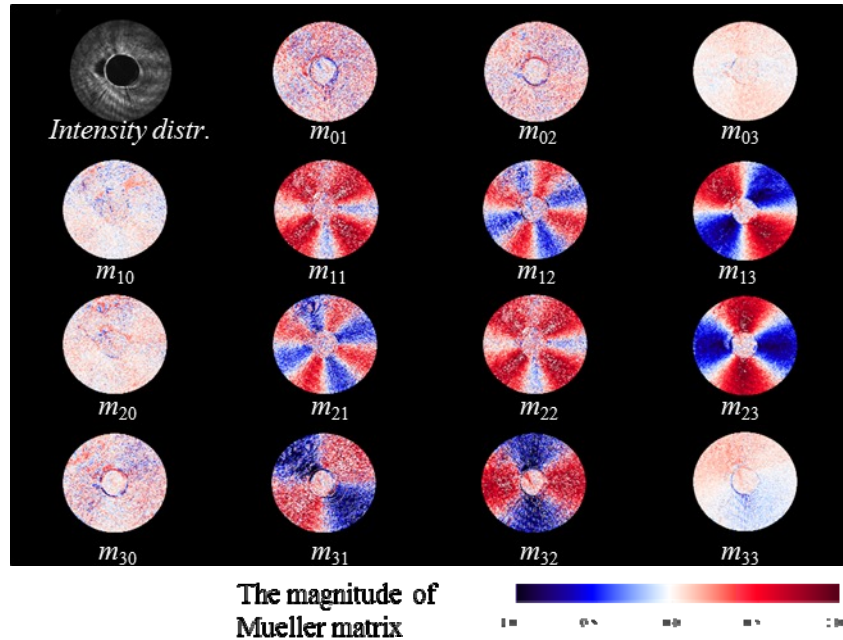


Fig.5 Mueller matrix distribution of axially symmetric quarter wave plate

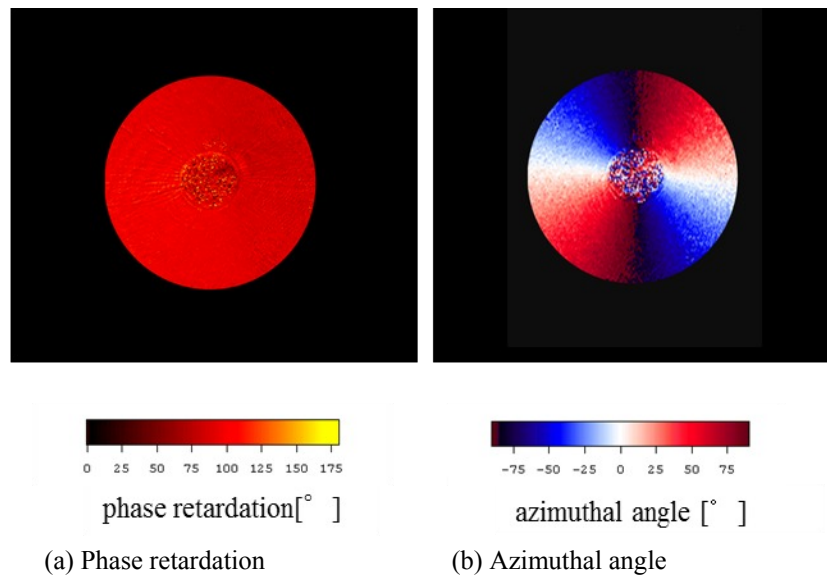


Fig.6 Birefringence properties of achromatic axially symmetric quarter wave plate

The color level is represented the magnitude of Mueller matrix from -1 to 1. The Mueller matrices distribution in Fig. 5 is normalized by  $m_{00}$  and  $m_{00}$  represents the intensity distribution. In these results, the magnitude of Mueller matrix components  $m_{01}$ ,  $m_{02}$ ,  $m_{03}$ ,  $m_{10}$ ,  $m_{20}$ ,  $m_{30}$  and  $m_{33}$  are almost zero. In addition, the Mueller matrix is symmetric. The Mueller matrix components  $m_{11}$  and  $m_{22}$  are also same in magnitude, and the Mueller matrices components  $m_{12}$ ,  $m_{13}$ , and  $m_{23}$  are almost equal in magnitude of the components  $m_{21}$ ,  $m_{31}$ , and  $m_{32}$  but opposite in sign, respectively. These results are in good agreement with theoretical values as shown in Eq. 2 when the  $\Delta$  equals  $90^\circ$ . Distributions of the phase retardation and the azimuthal angle are determined from Mueller matrix components such as  $m_{13}$ ,  $m_{23}$ , and  $m_{33}$ . Figure 6

shows the distribution of the phase retardation and the azimuthal angle, respectively. The phase retardation equals  $90^\circ$  and the azimuthal angle changes axially-symmetrically. From the histogram of the phase retardation, the center of the histogram is  $92^\circ$  and the dispersion in the histogram is  $\pm 9^\circ$ , approximately. The center of the histogram is corresponding with theoretical result since the theoretical result is  $89.7^\circ$ . When the slope angle is  $44.5^\circ$ , the phase retardation becomes  $93^\circ$ . According to this consideration, the wave plate works according to our calculations. Moreover, we investigated the reason for the dispersion in the histogram. It was clear that the concave conical surface has errors in the slope angle  $\beta$  from  $-0.2^\circ$  to  $0.2^\circ$ . If we can polish more precisely, the dispersion in the histogram will likely be smaller.

## 7. CONCLUSIONS

In this paper, we have demonstrated an achromatic axially symmetric wave plate based on Fresnel reflections. In experiments, we fabricated the wave plate using  $\text{SiO}_2$  with a glass lathe and polishing. The wave plate generates the state of polarization of an axially symmetric polarized beam. In addition, we have experimentally evaluated the wave plate using a dual rotating Mueller matrix polarimeter. The distributions of phase retardation and azimuthal angle are in good agreement with the theoretical values. Moreover, we investigated the phase retardation distribution of the wave plate. As this result, we found that the slope angle has slight errors from  $-0.2^\circ$  to  $0.2^\circ$  on the concave conical surfaces. The achromatic axially symmetric wave plate will be improved by introducing more precise polishing.

### Acknowledgement:

This work was partially supported by a Japan Science and Technology Agency, Adaptable and Seamless Technology transfer Program through target driven R&D for number AS242Z01381K.

## REFERENCES

- [1] Dennis, M. R., O'Holleran, K. and Padgett, M. J. [singular optics : optical vortices and polarization singularities, Progress in Optics, 53], Elsevier, Amsterdam, 293–363, (2009).
- [2] Zhan, Q., “Cylindrical vector beams: from mathematical concepts to applications” *Advances in Optics and Photonics*, 1, 1-57 (2009).
- [3] Kathleen Youngworth and Thomas Brown, “Focusing of high numerical aperture cylindrical-vector beams” *Opt. Express*, 7, 77-87 (2000).
- [4] Fontana, J.R. and Pantell, R. H., “A High-Energy Laser Accelerator for Electrons Using the Inverse Cherenkov Effect” *J.Appl. Phys.*, 54, 4285-4288 (1983).
- [5] Kraus, M, Ahmed, M.A., Michalowski, A., Voss, A., Weber, R., and Graf, T., “Microdrilling in steel using ultrashort pulsed laser beams with radial and azimuthal polarization” *Opt. Express*, 18, 22305-22313 (2010).
- [6] Rittweger, E., Han, K. Y., Irvine, S. E., Eggeling, C., and Hell, S. W., “STED microscopy reveals crystal color centres with nanometric resolution,” *Nature Photonics*, 3, 144–147 (2009).
- [7] Gahagan, K. T. and Swartzlander Jr., G. A. “Optical vortex trapping of particles”, *Opt. Lett.* 21, 827-829 (1996).
- [8] Gibbons, W. M., Shannon, P. J., Sun, S. T., Swetlin, B. J., “Surface-mediated alignment of nematic liquid crystals with polarized laser light” *Nature*, 351, 49-50(1991).
- [9] McEldowney, S.C., Shemo, D.M. and Chipman, R.A, “Vortex retarders produced from photo-aligned liquid crystal polymers” *Opt. Express*, 16, 7295-7308 (2008).
- [10] Ohtera, Y., Sato, T., Kawashima, T., Tamamura, T., and Kawakami, S., “Photonic crystal polarization splitters,” *Electron. Lett.* **35**, 1271–1272 (1999).
- [11] Bomzon, Z., Kleiner, V., and Hasman, E., “Formation of radially and azimuthally polarized light using space-variant subwavelength metal stripe gratings,” *Appl. Phys. Lett.* 79, 1587–1589 (2001).
- [12] Beresna, M., Gecevicius, M., Kazansky, P.G., and Gertus, T., “Radially polarized optical vortex converter created by femtosecond laser nanostructuring of glass” *Appl. Phys. Lett.* 98, 201101-201103 (2011).
- [13] Kozawa, Y., and Sato, S., “Single higher-order transverse mode operation of a radially polarized Nd:YAG laser using an annularly reflectivity-modulated photonic crystal coupler,” *Optics Letters*, 33, 19, pp. 2278-2280 (2008).

- [14] Wakayama, T., Komaki, K., Otani, Y., Yoshizawa, T., “Achromatic axially symmetric wave plate”, *Optics Express*, 20, 28, 29260-29265 (2012).
- [15] Wakayama, T., Otani, Y., Yoshizawa, T., “An interferometric observation of topological effect by novel axially symmetrical wave plate”, *Proc SPIE*, 849306, 849306-1~ 849306-8 (2012).
- [16] Mooney, F., ”A modification of the Fresnel rhomb,” *JOSA*, 42,3,181-182(1952).
- [17] M. Born and E. Wolf, [ *Principle of Optics* 7<sup>th</sup> edition], Cambridge Univ. press. UK, (1999).